

GNSS observations of deep convective time scales in the Amazon

D. K. Adams,^{1,3} Seth I. Gutman,² Kirk L. Holub,² and Dulcineide S. Pereira⁴

Received 05 April 2013; revised 14 May 2013; accepted 16 May 2013.

[1] In the tropics, understanding the shallow-to-deep transition and organization of convection on the mesoscale is made difficult due to the paucity of long-term high spatial/temporal resolution data. In this paper, data from the world's first long-term equatorial Global Navigational Satellite System meteorological station in Manaus (Central Amazon) is used to create a new metric, a water vapor convergence time scale, to characterize the temporal evolution of deep convection over a tropical continental region. From 3.5 years of data, 320 convective events were analyzed using a compositing analysis. Results reveal two characteristic time scales of water vapor convergence; an 8 h time scale of weak convergence and 4 h timescale of intense water vapor convergence associated with the shallow-to-deep convection transition. The 4 h shallow-to-deep transition time scale is particularly robust, regardless of convective intensity, seasonality, or nocturnal versus daytime convection. This new result provides a useful metric for both high resolution and global climate models to replicate. **Citation:** Adams, D. K., S. I. Gutman, K. L. Holub, and D. S. Pereira (2013), GNSS Observations of Deep Convective Time scales in the Amazon, *Geophys. Res. Lett.*, 40, doi:10.1002/grl.50573.

1. Introduction

[2] Understanding and modeling of the transition from shallow to organized deep convection is a particularly vexing problem in tropical meteorology [Betts and Jakob, 2002; Wu et al., 2009]. Deep precipitating convection, whose origins are as incipient cumuli, a small-scale phenomenon, temporally, of tens of minutes and, spatially, of kilometers, can become organized and experience upscale growth into mesoscale convective systems with scales of hours to a day and of 100 km to 1000 km. Furthermore, given the weak rotational constraint near the equator, heating perturbations resulting from deep precipitating convection are quickly redistributed to scales much larger than 1000 km by gravity wave dynamics [Mapes, 1997]. For what may be essentially considered a single evolving phenomenon, deep convection covers a range of spatial and temporal scales

which are challenging to capture observationally and to represent in numerical models [Mapes et al., 2009; Moncrieff et al., 2012; Zhang et al., 2013]. Apart from scale issues, very complex interactions/feedbacks exist between tropical convection and water vapor (wv) fields (see Sherwood et al. [2009] for a review). Tropical deep convection depends on the spatial and temporal distribution of wv, yet deep convection is also critical in determining this distribution [Grabowski and Moncrieff, 2004]. For example, it has been pointed out that moist regions experience more deep convection, a positive feedback, though precipitating convection ultimately dries the atmosphere [Grabowski and Moncrieff, 2004]. Furthermore, the vertical distribution of wv can influence cumulus dynamics and the shallow-to-deep transition through entrainment of dry air with its deleterious effects on buoyancy [Khairoutdinov and Randall, 2006; Wu et al., 2009].

[3] Unraveling the complex nature of the shallow-to-deep transition and deriving useful metrics that characterize its temporal evolution, long-term (i.e., years), high frequency measurements (≤ 30 min) at spatial resolutions of kilometers are necessary. However, it is precisely at this scale that long-term observations are lacking in the tropics. Satellite observations of clouds and column wv are crucial for characterizing the evolution of tropical convection; nevertheless, these platforms have neither the spatial nor temporal resolution for capturing wv/convection interactions that cover the cumulus stage, the shallow-to-deep transition, and upscale growth to mesoscale convective systems. Moreover, satellite wv measurements from IR radiometers are limited to clear-sky conditions [Divakarla et al., 2006], and satellite microwave radiometers are less reliable over land [Deeter, 2007]. Within the last two decades, ground-based Global Navigational Satellite System (GNSS) meteorology has offered high frequency (as frequent as 5 min), all-weather, precipitable water vapor (PWV) values with 1 to 2 mm accuracy relative to radiosondes and radiometers [Mattioli et al., 2007; LeBlanc et al., 2011].

[4] Although PWV is only an integral measure providing no vertical humidity structure, it has proven valuable for deriving empirical precipitation relationships [Zeng, 1999; Bretherton et al., 2004] and for theoretical work on deep convective organization in the tropics [Neelin et al., 2009; Peters et al., 2009]. The time evolution of GNSS-derived PWV has been used in studies of deep convection [Mazany et al., 2002; Kursinski et al., 2008], but never within the equatorial tropics. In this paper, we present a new application of GNSS ground-based PWV, namely, examining the wv convergence time scales for a tropical continental region, the central Amazon. The motivations are twofold: (1) to introduce the GNSS-derived wv convergence time scale and, (2) to characterize deep convective events for a tropical continental regime using this metric. Many different time scales exist for deep convection, and time scale

¹Centro de Ciencias de la Atmósfera, Universidad Nacional Autónoma de México, Distrito Federal, México.

²Earth System Research Laboratory, National Atmospheric and Oceanic Administration, Boulder, Colorado, USA.

³Programa em Clima e Ambiente, Universidade do Estado do Amazonas, Manaus, Amazonas, Brazil.

⁴Instituto Federal de Educação, Ciência e Tecnologia, Manaus, Amazonas, Brazil.

Corresponding author: D. K. Adams, Centro de Ciencias de la Atmósfera, Universidad Nacional Autónoma de México, Circuito Exterior s/n, Ciudad Universitaria, Del. Coyoacán, 04510 México D.F., México (dave.k.adams@gmail.com)

analysis lies at the root of understanding which physical processes are dominant [Mapes *et al.*, 2009; Hohenegger and Stevens, 2013]. For example, recent work by Hohenegger and Stevens [2013] utilizes time scale analysis to determine which process dominates convective outbreaks, cumulus congestus moisture preconditioning or dynamically forced wv convergence, the latter mechanism being dominant.

[5] Long-term, continuous observations/statistics are, however, absolutely necessary to gain further insight into wv/convection interactions. Here, we employ 3.5 years of PWV data from the world’s first equatorial GNSS meteorology station in Manaus, Brazil to examine wv convergence time scales. In what follows, we present the derivation and underlying assumptions for relating the time evolution of PWV to wv convergence. The methodology, study area, and data employed in developing the deep convective climatology are then presented. Application of this time scale to Amazon convection is discussed and future directions of GNSS-based studies in the tropics close the paper.

2. Derivation, Study Area, Data, and Methodology

2.1. Derivation

[6] Assuming a wv scale height of 2.5 km and average satellite elevation angle of 30°, GNSS-derived PWV is representative of a cone of view of radius of approximately 10 km, and the derivation that follows is based on this scale. The local time rate of change (i.e., Eulerian framework) of PWV measured with GNSS relates directly to wv convergence above the antenna and, hence, to deep convection. Convective updrafts bring the rising moist air toward saturation, cloud formation and, finally, precipitation. The temporal evolution of integrated (or column) wv, ignoring horizontal condensate advection, is related to wv convergence through the water conservation equation (per unit area)

$$\frac{\partial}{\partial t}(\text{IWV}) + \frac{\partial}{\partial t} \int q_c \frac{dp}{g} + \nabla \cdot \int q \vec{V} \frac{dp}{g} = E - P. \quad (1)$$

where IWV is the integrated (or column) wv. Conversion of IWV to PWV, as most commonly defined, requires division by liquid water density, ρ_w ;

$$\text{PWV} = \frac{1}{\rho_w} \int q \frac{dp}{g} = \frac{\text{IWV}}{\rho_w}. \quad (2)$$

[7] In both equations (1) and (2), p is pressure, g , gravity, q specific humidity, q_c , condensate per unit moist air \vec{V} , the horizontal wind vector and integration is over the depth of the atmospheric column. At this spatial scale, local evaporation is negligible compared to the wv convergence term; i.e., $E \ll \nabla \cdot \int q \vec{V} \frac{dp}{g}$. As the shallow-to-deep transition begins, and prior to onset of heavy precipitation, P , the time rate of change of IWV is determined by wv convergence and the generation of convective cloud water, $\frac{\partial}{\partial t} \int q_c \frac{dp}{g}$. Furthermore, if it is assumed that the time derivative of the cloud term is small compared to that of IWV, (see discussion below for more on this assumption), then the time rate of change of PWV is a measure of wv convergence in the column

$$\left| \frac{\partial}{\partial t}(\text{PWV}) \right| \sim \left| \nabla \cdot \frac{1}{\rho_w} \int q \vec{V} \frac{dp}{g} \right|. \quad (3)$$

In this respect, the time evolution of GNSS-derived PWV can provide a useful measure of wv convergence time scales. The fact that GNSS PWV is all-weather and high frequency is particularly advantageous given that rapidly evolving cloudy and rainy conditions are precisely those of interest. Although the GNSS spatial scale is too coarse to resolve individual cumulus, a small-scale field of evolving cumulus is resolved as well as the transition to growing cumulonimbus events at the large end.

2.2. Study Site

[8] The GNSS meteorological station INPA functioned from July 2008 to December 2011 as part of the National Oceanic and Atmospheric Administration/Earth System Research Laboratory (NOAA/ESRL) Ground-Based GPS Meteorological Network located at the National Institute for Amazon Research/Large Scale Biosphere-Atmosphere Experiment (INPA/LBA) in Manaus, Brazil (−2.61°S, −60.21°W). In the central Amazon, annual rainfall totals are copious (~ 2500 mm yr^{−1}), occurring throughout the year, but most heavily from January to April, with a distinct dry season from July to September [Machado *et al.*, 2004] (see Figure 1). Diurnal forcing is strong, as with most continental tropical regimes, and a notable afternoon maximum is observed (see Figure 1).

2.3. Data and Methodology

[9] To examine convective time scales, a deep convective “climatology” was developed utilizing surface meteorological variables, cloud-top temperature (CTT), and GNSS-derived PWV. The INPA site consisted of a dual frequency, geodetic-grade GNSS receiver/antenna and meteorological station measuring pressure, temperature, relative humidity, winds, and precipitation at 1 min sampling frequency. NOAA/ESRL processed the GNSS data in near real time (2 h latency) providing PWV values every 30 min. GOES 10/12 Channel 4 IR provided the brightness temperature (i.e., CTT) from near nadir with 4 km × 4 km resolution at every 15 or 30 min. To coincide with the “cone of observation” of GNSS PWV, CTT was averaged for a 4 × 4 pixel box (16 km × 16 km) centered over INPA. To identify the convective events comprising the climatology, several criteria were employed. All convective events met the following criteria: (1) a precipitous drop in CTT of at least 50 K in less than 2 h falling to below 235 K, (2) a concomitant ramp up of PWV to a maximum value occurring within approximately 1 h of minimum CTT, and (3) precipitation and/or the identification of precipitation-driven downdrafts with their unmistakable temperature and wind speed signature. A surface temperature drop of more than 3 K in less than 30 min accompanying a rapid jump in wind speed of 3 m/s were considered convective-scale downdraft and, hence, nearby precipitation (see Figure 2). Advancing cirrus shields or regions of stratiform precipitation, which could, in theory, lead to CTT behavior similar to deep convective events, would not be included in this climatology because all three criteria simply could not be met in the equatorial tropics. The time evolution of PWV and meteorological variables were composited according to the criteria of interest. The time series composites, centered on the maximum PWV observed with deep cloud formation and precipitation, were extended 14 h prior to and after the convective event.

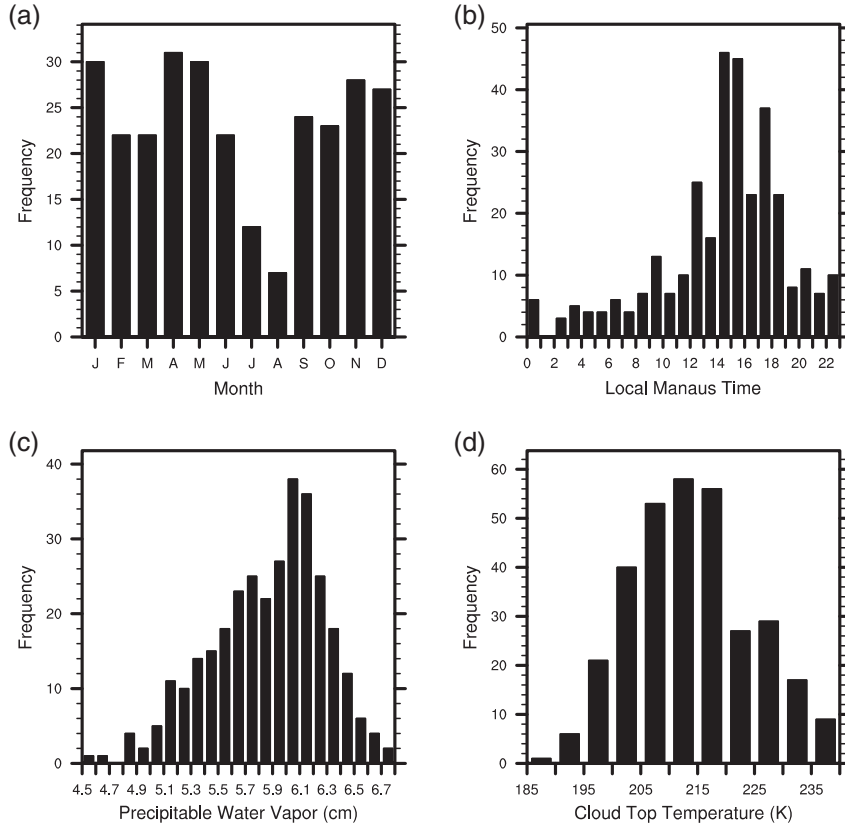


Figure 1. Histograms of the distribution of deep convective events based on the (a) annual cycle, (b) diurnal cycle, (c) maximum PWV, and (d) minimum CTT. The annual cycle was derived from only three complete years so as not to bias the frequencies.

3. Results

[10] For the 3.5 year period of observation, 320 events were classified as deep precipitating convection. Figure 1 characterizes the distribution of these events with respect to season, time of day, maximum PWV, and minimum CTT. To evaluate characteristic wv convergence time scales, any number of criteria may be employed (e.g., precipitation intensity, degree of organization, propagating versus non-propagating, etc.). Here, however, as a “proof of concept,” we evaluate wv convergence based solely on the criteria in Figure 1. The composite of all 320 events (Figure 2) reveals two characteristic time scales. First, a slow, quasi-linear time scale of approximately 8 h is observed. Here, local evaporation most probably plays a greater role relative to wv convergence, particularly given the strong surface forcing during the diurnal cycle. A second rapid nonlinear ramp up of approximately 4 h is also observed. Within the latter, the transition from shallow-to-deep precipitating convection occurs. Around 4 h prior to heavy precipitation and maximum PWV , CTT decreases slowly for approximately 2 h as convective clouds deepen. This is followed by a precipitous drop in CTT as convective cells grow rapidly and then precipitate. As noted above in section 2.1, $\frac{\partial}{\partial t}(PWV)$, is not the same as wv convergence given wv sink terms such as cloud formation and precipitation. At large space (>100 km) and time scales (>1 day), the cloud term can be ignored [Peixoto and Oort, 1992], but not necessarily for deep cumulonimbus at the scale of interest here (~ 20 km, < 1 h). However, it is apparent from Figure 2 that PWV grows in an accelerated

fashion despite rapid cloud growth (i.e., a large drop in CTT) and even precipitation. Only as heavy precipitation occurs around $t = 0$ and CTT reaches its minimum does PWV begin to decrease. This becomes more apparent when directly plotting $\frac{\partial}{\partial t}(PWV)$ and $\frac{\partial}{\partial t}(CTT)$ as functions of time (Figure 3), where $\frac{\partial}{\partial t}(CTT)$ serves as a rough measure of cloud growth rate. The entire event composite, as well as dry versus rainy season composites, shows accelerated cloud growth between approximately $t - 3$ and a maximum at $t - 1$ h which occurs simultaneously with large increases in $\frac{\partial}{\partial t}(PWV)$. If the cloud term were considerable, one would expect a leveling off or decrease in $\frac{\partial}{\partial t}(PWV)$, which is not observed, thereby, lending credence to our approximation in equation 3.

[11] From Figure 3, the 4 h wv convergence time scale associated with the shallow-to-deep transition is nearly identical, independent of season. Nevertheless, one may argue that the shallow-to-deep transition time scale may be sensitive to atmospheric stability, to the vertical profile of wv, to diurnal forcing, or to a myriad of other environmental factors. On the other hand, wv convergence time scales could also differ with respect to observed characteristics such as convective intensity, degree of organization, lifetime, propagating versus non-propagating, etc. With this in mind, we composited convective events as nocturnal versus diurnal and as a function of maximum PWV; these represent external factors/forcing. In terms of convective characteristics, minimum CTT represented “intensity”. The robustness of the wv convergence time scale is revealed in these differing composites.

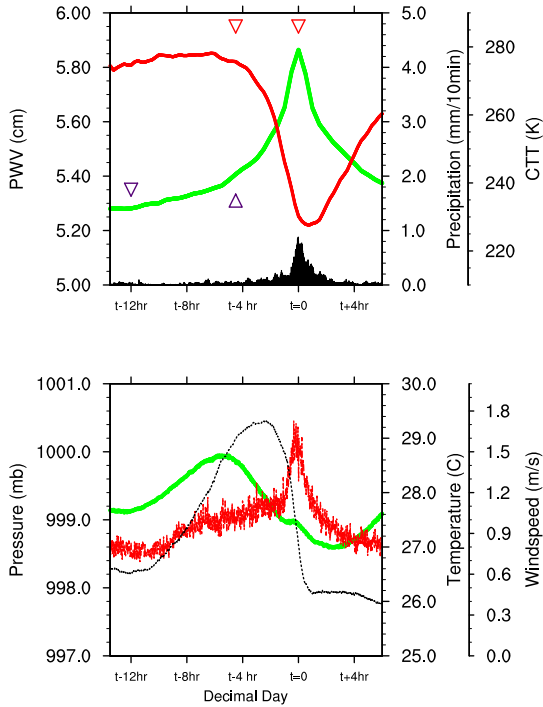


Figure 2. Composite time series of all 320 convective events. The upper panel contains PWV (green line), CTT (red line), and precipitation (black bars). The blue and red triangles represent the 8 and 4 h wv convergence time scales, respectively. The lower panel contains surface meteorological data; pressure (green line), temperature (black line), and wind speed (red line).

[12] In order to more rigorously define the shallow-to-deep transition based on the observed variables, several criteria were utilized. The shallow-to-deep transition was assumed to begin at maximum CTT that coincides with continuously positive values of $\frac{\partial}{\partial t}(\text{PWV})$ and continuously negative values of $\frac{\partial}{\partial t}(\text{CTT})$ until $t = 0$. In Figure 4, which contains the plots of $\frac{\partial}{\partial t}(\text{PWV})$ versus $\frac{\partial}{\partial t}(\text{CTT})$ in accordance with the above-mentioned categories, the shallow-to-deep transition commencement is indicated by the black vertical line. From Figure 2, there is an apparent diurnal signal in the data. To demonstrate the wv vapor convergence time scale observed is not a relict of the diurnal cycle, daytime versus nocturnal events were examined. Diurnal (1 PM to 7 PM LST) versus nocturnal (2 AM to 10 AM LST) events were composited, the underlying assumption being that forcing differs as a function of time of day and may be reflected in the wv vapor convergence time scale. Clearly, forcing associated with the solar cycle is irrelevant for nocturnal events which are most likely associated with formation along convective outflow boundaries, propagating squall lines or nocturnal mesoscale convective systems. Though the forcing is most assuredly different, both nocturnal and diurnal composites contain the 8 h slow wv convergence (not shown). The shallow-to-deep transition appears to begin closer to $t - 6$ h, but this may well be a result only of our chosen criteria. The rapid increase in wv vapor convergence at $t - 4$ h is still observed as well as the $t - 1$ h wv convergence maximum.

[13] To emphasize possible variations in the wv convergence time scale, the extreme ends in the approximately

normal distribution in maximum PWV and minimum CTT (top/bottom 15%, $N = 48$) were composited (Figure 4). In the case of maximum PWV, events were composited as dry events with maximum PWV less than 5.4 cm and humid events with maximum PWV greater than 6.25 cm. For minimum CTT, convective events were composited as weak ($\text{CTT} > 226$ K) and strong ($\text{CTT} < 205$ K). As with diurnal versus nocturnal convection, weak positive wv convergence occurs for approximately 8 h (not shown), followed by accelerated wv convergence from 4 h to 1 h prior to deep convection. Deeper convection ($\text{CTT} < 205$ K) and moisture environments ($\text{PWV} > 6.25$ cm) experience greater wv vapor convergence, but the temporal evolution is nearly identical.

[14] In all cases presented, wv convergence indicates there are two time scales present, essentially, 12 h of positive convergence, the first 8 h indicating weak wv convergence followed by rapid acceleration around 4 h, peaking in intensity at 1 h prior to deep precipitating convection. The latter 4 h time scale contains the shallow-to-deep transition and growth to deep precipitating cumulonimbus. Given the similar temporal evolution of wv convergence for diurnal and nocturnal convection, the 12 h period is not reflective of the diurnal cycle. It should be noted that the nocturnal sample size is small ($N = 47$), and the slow 8 h time scale observed in these nocturnal events is difficult to attribute to a specific physical mechanism with precisely this 8 h time scale. Water vapor convergence varies in intensity as a function of the criteria being examined, moister environments, and deeper convection being associated with the strongest wv convergence.

[15] To the extent that this climatology represents the mean and variability of this tropical continental convection, the temporal evolution of water vapor convergence is strikingly robust. Granted, we have employed rather gross measures of environmental conditions, and more sophisticated criteria need to be considered to ascertain the dependence on external factors (e.g. stability and tropospheric humidity) as shown in *Wu et al.* [2009]. Likewise, in a future study, shallow-to-deep transition time scales will be observed for propagating systems, and an estimate will be made for their associated cloud condensate advection term.

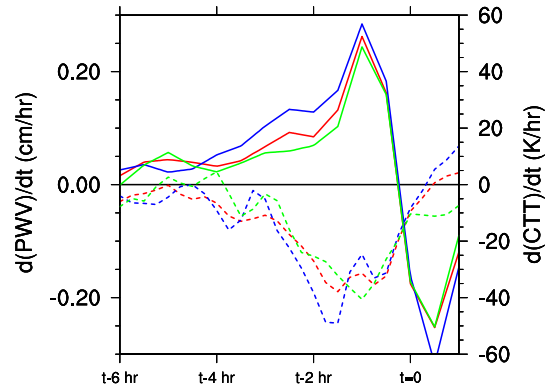


Figure 3. A time series of the time derivatives of PWV (solid lines) and CTT (dashed lines) for the entire composite, $N = 320$, (red) the wet season (January to April), $N = 105$ (green) and the dry season (July to September), $N = 51$, (blue). The time series begins at $t - 6$ h only for clarity of presentation.

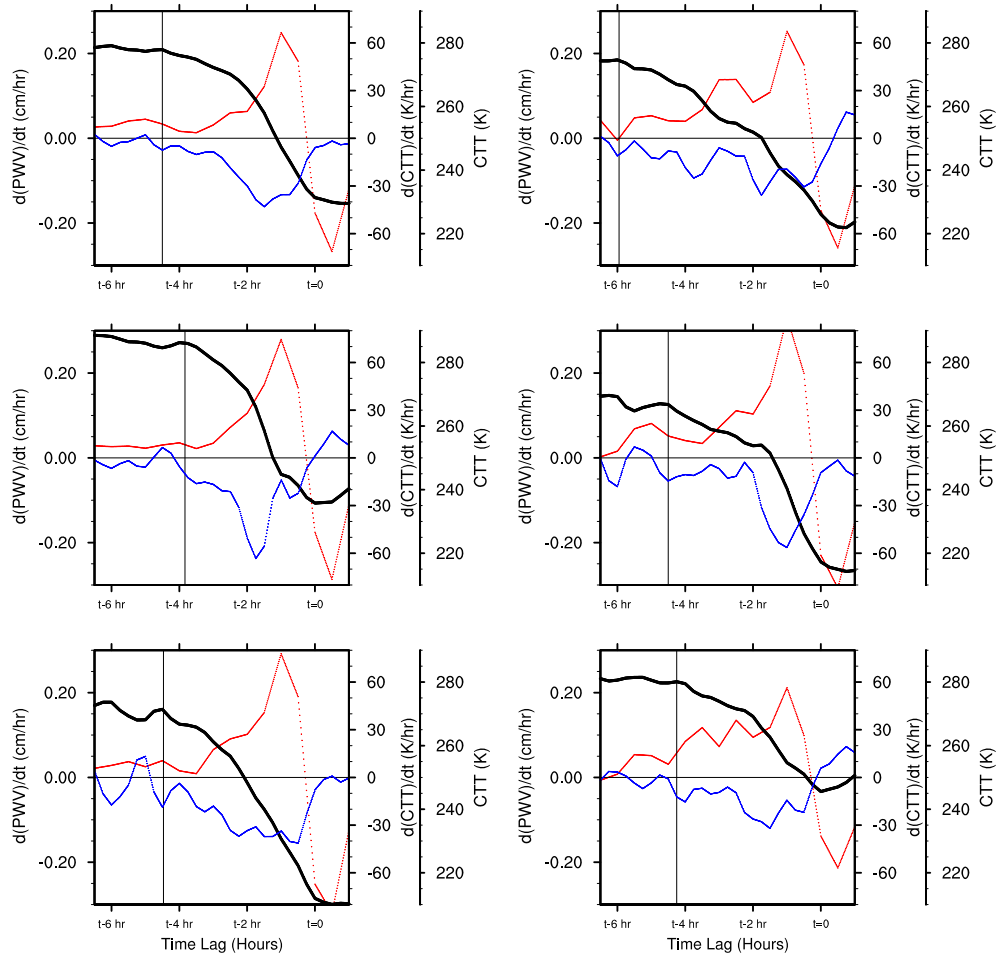


Figure 4. A time series of CTT (black lines) and of the time derivative of PWV (red lines) and the time derivative of CTT (blue lines). The upper panels represent diurnal events, $N = 178$, (left panel) versus nocturnal events, $N = 47$ (right panel). The middle panels represent dry events, $N = 48$, (left panel) versus moist events, $N = 48$ (right panel). The lower panels represent more intense events, $N = 48$, (left panel) versus less intense events, $N = 48$ (right panel). The thin vertical black line represents the start of the shallow-to-deep transition (see text). The time series begins at $t - 6$ h only for clarity of presentation.

4. Conclusion

[16] This study represents the first small-scale, long-term, in situ, observational study of PWV/convection behavior in an equatorial continental site. Up to the present, the majority of tropical shallow-to-deep transition studies have been modeling efforts. This study provides well-needed observational evidence for model-derived time scales and, hence, offers a valuable metric. GNSS PWV given its all-weather capacity and lack of instrument drift provides a unique platform for tropical convective studies and has now recently expanded into the tropics. COCONet [Braun *et al.*, 2012] will consist of 130 GNSS meteorology stations for studying Caribbean climate and meteorology. Furthermore, Adams *et al.* [2011a, 2011b] created the Amazonian Dense GNSS Meteorological network (April 2011 to April 2012), the first of its kind in the deep tropics, consisting of 20 GNSS meteorological stations over a $100 \text{ km} \times 100 \text{ km}$ area centered in Manaus to examine wv/convection relationships at a higher spatial/temporal resolution. We intend this paper to be a timely contribution particularly in light of the intensive field campaigns

in and around Manaus scheduled for next year, namely, GoAmazon2014 (<http://campaign.arm.gov/goamazon2014/>) and GPM-CHUVA (<http://chuvaproject.cptec.inpe.br/portal/noticia.ultimas.logic>). These field campaigns will provide an unprecedented opportunity to examine the evolution of deep convection in the equatorial tropics.

[17] **Acknowledgments.** We would like thank INPA/LBA, Brazil, for financial support (Antônio Manzi, Hilândia Cunha). For technical support, we thank Cicero Leite (INPA/LBA) and UNAVCO, in particular, Jim Normandeau. We thank Yolande Serra for comments on a previous draft and Luiz Machado and Roberto Freitas (INPE/DSA, Brazil) for GOES data. Special thanks go to Rob Kursinski and Rick Bennett for encouraging/supporting this project from its inception.

References

- Adams, D. K., *et al.* (2011a), A dense GNSS meteorological network for observing deep convection in the Amazon, *Atmos. Sci. Let.*, *12*, 207–212, doi:10.1002/asl.312.
- Adams, D. K., R. M. S. Fernandes, and J. M. F. Maia (2011b), GNSS precipitable water vapor from an Amazonian rain forest flux tower, *J. Atmos. Oceanic Technol.*, *28*, 1192–1198.
- Betts, A. K., and C. Jakob (2002), Study of diurnal convective precipitation over Amazonia using a single column model, *J. Geophys. Res.*, *107*(D23), 4732, doi:10.1029/2001JD002264.

- Braun, J. J., G. Mattioli, D. C. E. Calais, M. Jackson, R. Kursinski, M. Miller, and R. Pandya (2012), Multi-disciplinary natural hazards research initiative begins across Caribbean basin, *EOS. Trans. AGU*, 93(9), 89–90, doi:10.1029/2012EO090001.
- Bretherton, C. S., M. E. Peters, and L. E. Back (2004), Relationships between water vapor path and precipitation over the tropical oceans, *J. Climate*, 17, 1517–1528.
- Deeter, M. (2007), A new satellite retrieval method for precipitable water vapor over land and ocean, *Geophys. Res. Lett.*, 34, L02815, doi:10.1029/2006GL028019.
- Divakarla, M. G., C. D. Barnett, M. D. Goldberg, L. M. McMillin, E. Maddy, W. Wolf, L. Zhou, and X. Liu (2006), Validation of atmospheric infrared sounder temperature and water vapor retrievals with matched radiosonde measurements and forecasts, *J. Geophys. Res.*, 111, D09S15, doi:10.1029/2005JD006116.
- Grabowski, W. W., and M. W. Moncrieff (2004), Moisture-convection feedback in the tropics, *Quart. J. Roy. Meteor. Soc.*, 130, 3081–3104.
- Hohenegger, C., and B. Stevens (2013), Preconditioning deep convection with cumulus congestus, *J. Atmos. Sci.*, 70(2), 448–464.
- Khairoutdinov, M., and D. Randall (2006), High-resolution simulation of shallow-to-deep convection transition over land, *J. Atmos. Sci.*, 63, 3421–3436.
- Kursinski, E. R., R. A. Bennett, D. Gochis, S. I. Gutman, K. L. Holub, R. Mastaler, C. M. Sosa, I. M. Sosa, and T. van Hove (2008), Water vapor and surface observations in northwestern Mexico during the 2004 NAME enhanced observing period, *Geophys. Res. Lett.*, 35, L03815, doi:10.1029/2007GL031404.
- LeBlanc, T., et al. (2011), Measurements of humidity in the atmosphere and validation experiments (MOHAVE)-2009: Overview of campaign operations and results, *Atmos. Meas. Tech.*, 4, 2579–2605.
- Machado, L. A. T., H. Laurent, N. Dessay, and I. Miranda (2004), Seasonal and diurnal variability of convection over the Amazonia: A comparison of different vegetation types and large scale forcing, *Theor. Appl. Climatol.*, 78, 61–77, doi:10.1007/s00704-004-0044-9.
- Mapes, B. (1997), *Equilibrium vs. activation controls on large-scale variations of tropical deep convection*, in *The Physics and Parameterization of Moist Convection*, edited by Smith, R. K., 321–358, Kluwer, Dordrecht, Netherlands.
- Mapes, B., R. Milliff, and J. Morzel (2009), Composite life cycle of maritime tropical mesoscale convective systems in scatterometer and microwave satellite observations, *J. Atmos. Sci.*, 66, 199–208.
- Mattioli, V., E. R. Westwater, D. Cimini, J. S. Liljegren, B. M. Lesht, S. I. Gutman, and F. J. Schmidlin (2007), Analysis of radiosonde and ground-based remotely sensed pwv data from the 2004 North Slope of Alaska Arctic Winter Radiometric Experiment, *J. Atmos. Ocean. Technol.*, 24, 415–431.
- Mazany, R. A., S. Businger, S. I. Gutman, and W. Roeder (2002), A lightning prediction index that utilizes GPS integrated precipitable water vapor, *Wea. Forecasting*, 17, 1034–1047.
- Moncrieff, M. W., D. E. Waliser, M. J. Miller, M. A. Shapiro, G. R. Asrar, and J. Caughey (2012), Multiscale convective organization and the YOTC virtual global field campaign, *Bull. Amer. Meteor. Soc.*, 93, 1171–1187.
- Neelin, J. D., O. Peters, and K. Hales (2009), The transition to strong convection, *J. Atmos. Sci.*, 66, 2367–2384.
- Peixoto, J. P., and A. H. Oort (1992), *Physics of Climate*, pp. 520, AIP Press, New York City.
- Peters, O., J. D. Neelin, and S. W. Nesbitt (2009), Mesoscale convective systems and critical clusters, *J. Atmos. Sci.*, 66, 2913–2924.
- Sherwood, S., R. Roca, T. Weckwerth, and N. Andronova (2009), Tropospheric water vapor, convection and climate: A critical review, *Rev. Geophys.*, 48, RG2001, doi:10.1029/2009RG000301.
- Wu, C.-M., B. Stevens, and A. Arakawa (2009), What controls the transition from shallow to deep convection? *J. Atmos. Sci.*, 66, 1793–1806.
- Zeng, X. (1999), The relationship among precipitation, cloud-top temperature, and precipitable water over the tropics, *J. Climate*, 12, 2503–2514.
- Zhang, C., J. Gottschalck, E. D. Maloney, M. Moncrieff, F. Vitart, D. E. Waliser, B. Wang, and M. C. Wheeler (2013), Cracking the MJO nut, *Geophys. Res. Lett.*, 40, 1223–1230, doi:10.1002/grl.50244.